Contents lists available at ScienceDirect

Computers & Graphics

journal homepage: www.elsevier.com/locate/cag

Discrete Orthogonal Structures

ARTICLE INFO

Article history:
Received March 30, 2023

Keywords: orthogonal meshes, orthogonal multi-nets, mesh optimization, principal meshes, developable surfaces, CMC surfaces

ABSTRACT

To represent smooth geometric shapes by coarse polygonal meshes, visible edges often follow special families of curves on a surface to achieve visually pleasing results. Important examples of such families are principal curvature lines, asymptotic lines or geodesics. In a surprisingly big amount of use-cases, these curves form an orthogonal net. While the condition of orthogonality between smooth curves on a surface is straightforward, the discrete counterpart, namely orthogonal quad meshes, is not. In this paper, we study the definition of discrete orthogonality based on equal diagonal lengths in every quadrilateral. We embed this definition in the theory of discrete differential geometry and highlight its benefits for practical applications. We demonstrate the versatility of this approach by combining discrete orthogonality with other classical constraints known from discrete differential geometry. Orthogonal multi-nets, i.e. meshes where discrete orthogonality holds on any parameter rectangle, receive an in-depth analysis.

1. Introduction

Representing smooth surfaces by coarse polygonal meshes in a visually pleasing way is a challenging task that is particularly important in Architectural Geometry [1]. There, visible edges of polygonal meshes often follow families of special curves in the underlying surface. Finding consistent discrete analogues of these curves is essential for the construction and optimization of the polygonal meshes. From a methodological perspective, there is a close relation to Discrete Differential Geometry [1, 2].

A property shared by the vast majority of curve networks of interest is orthogonality, examples being principal curvature lines, principal stress lines, the asymptotic lines in a minimal surface or geodesic lines in a developable surface. While the concept of orthogonality is straightforward in the smooth setting, it is not for discrete structures. Clearly, in a discrete version of an orthogonal curve network, not all angles can be 90°. For a fine mesh, they may be close to a right angle, but for coarser meshes this is certainly not true. Thus, the question of how to discretize orthogonality is a valid one. Within Discrete Differential Geometry, the predominant orthogonal structures are circular meshes [2] and conical meshes [3]. They come with an extensive theory but are only applicable to meshes with planar faces. Hence, they are always discrete principal curvature parametrizations.

A recent development in the realm of Discrete Differential Geometry is to define discrete structures through a pairing of meshes which has been used in [4, 5] to successfully discretize the system of confocal quadrics. The checkerboard pattern approach of [6, 7] following on earlier work by Kenyon [8] is equivalent to the mesh pairing and has been used to discretize isothermic surfaces in [9]. The mesh pairing approach to discrete principal curvature line parametrization generalizes and unifies the theory behind circular and conical meshes [10]. Similarly, the mesh pairing approach to Koenigs nets [11] generalizes and unifies the common discretizations of Koenigs nets by [12] and [13] as stated in [9]. This indicates the potential of the approach. However, using it for practical applications is tedious as one usually does not want to deal with two meshes at the same time representing the same shape. Taking the equivalent approach of checkerboard patterns, one is forced to work with parallelograms in every second face and boundary matching becomes particularly difficult. We overcome these difficulties by using the mesh pairing approach to first model rhombic nets. Then, by interpreting the two rhombic nets as the two diagonal nets of an orthogonal net, we obtain a natural discrete version of orthogonality. It boils down to the simple condition that the diagonals in every quadrilateral are of equal length. The same orthogonality condition has been used in [14, 15] but did not receive an in-depth treatment there.

This discrete version of orthogonality has the following properties which make it attractive for applications:

- It is applicable to arbitrary quad meshes.
- One works with only one mesh in contrast to the mesh pairing approach and there are no problems with boundary alignment.
- It is a simple distance constraint which is easily incorporated into numerical optimization. Being a quadratic constraint, it works well with Gauß-Newton algorithms. There is no need to use additional auxiliary variables to achieve quadratic constraints (which would be necessary for circular meshes [2] or conical meshes [3]).

The contribution of this paper is twofold. On the one hand, we motivate the orthogonality constraint through rhombic mesh pairings (Section 2) and discuss the appearance of this constraint in classical geometry (Section 3). We find that *Ivory's Theorem* guarantees the existence of special structures, which we refer to as orthogonal multi-nets. These orthogonal multi-nets and their design space are studied in Section 3.1 and 3.2. A local version of multi-nets can be used as a regularizer in optimization methods as described in 3.3. On the other hand, we present an overview of the different use-cases of the orthogonality constraint showcasing the versatility of the approach in Section 4. The discrete structures accessible through this approach include principal curvature lines, orthogonal geodesic nets and orthogonal Chebyshev nets on developable surfaces, asymptotic nets on minimal surfaces, principal symmetric nets on CMC surfaces and principal stress nets, see Tab. 1.

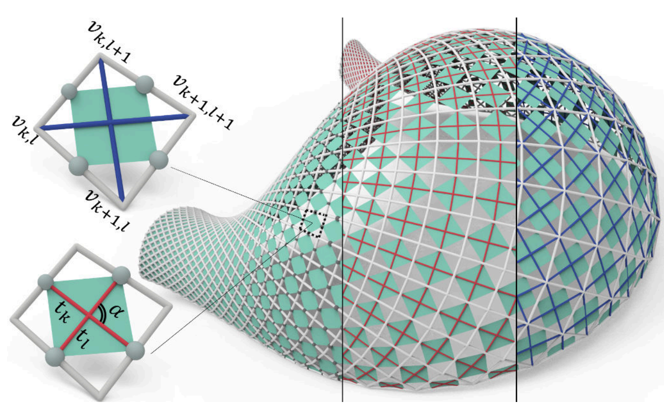

Fig. 1. Discrete orthogonality of the light grey mesh is characterized via the two diagonal meshes (blue). In each face of the discrete orthogonal mesh the two diagonals are of equal length and thus form a rhombic mesh pairing. The medial lines of the orthogonal mesh are depicted in red. They intersect orthogonally in every face. The zoom highlights the equivalence of orthogonal medial lines and diagonals of equal length.

2. Rhombic mesh pairings and discrete orthogonality

Throughout this paper we deal with quadrilateral meshes of grid-combinatorics that are parameterized over a rectangular portion of the $\mathbb{Z}^2$-lattice. However, different regular meshes can be joined to form patches with singular vertices. We denote a vertex of a mesh by $v_{k,l}$ and its corresponding neighbours by $v_{k\pm1,l}, v_{k,l\pm1}$. We refer to the polyline parameterized by $i \mapsto v_{i,j}$ as the j-th horizontal parameter line H_j of a mesh and likewise to V_k as the k-th vertical parameter line. We consider a mesh to be a discretization of a network of smooth curves on a surface to which we refer as net.

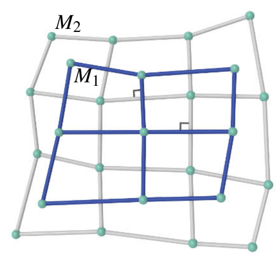

Fig. 2. The blue mesh M_1 is dual to the grey mesh M_2. Together they constitute an orthogonal mesh pairing as corresponding edges are orthogonal.

Mesh pairing. A mesh pairing is defined via two combinatorially dual meshes, compare Fig. 2. Let $M_1 : G \to \mathbb{R}^3$ be a mesh defined on a quad graph G and let $M_2 : G^* \to \mathbb{R}^3$ be a mesh defined on the dual graph G^*. We call (M_1, M_2) a mesh pairing. Every vertex of M_1 can be associated with a face of M_2 and vice versa. Moreover, for every edge of M_1 there is a corresponding edge of M_2. We view both meshes as a discretization of the same smooth surface. Geometric properties related to first order derivatives are encoded in the relation of corresponding edges, while properties related to second order derivatives like conjugacy are encoded in the faces of the meshes and can be associated with the corresponding vertices [6]. For example, one can say that a mesh pairing (M_1, M_2) is orthogonal if corresponding edges of M_1 and M_2 are orthogonal. The mesh pairing is conjugate if all faces of M_1 and M_2 are planar, which is the usual definition for discrete conjugacy of a quad mesh, see [2]. In that case, the face normals of M_1 are the vertex normals of M_2 and vice versa. However, since we want to deal with one mesh only eventually, we are not interested in orthogonal mesh pairings but in rhombic mesh pairings.

Definition 1. *A mesh pairing (M_1, M_2) is rhombic, if and only if corresponding edges of M_1 and M_2 are of equal length.*

The connection to orthogonality is motivated by the following lemma.

Lemma 2. *The parametrization of a smooth surface $\phi : \mathbb{R}^2 \to \mathbb{R}^3$ is orthogonal (i.e. $\partial_u\phi \perp \partial_v\phi$) if and only if the diagonal parametrization $\psi(u, v) := \phi(u+v, u-v)$ is rhombic (i.e. $\|\partial_u\psi\| = \|\partial_v\psi\|$).*

A given mesh pairing (M_1, M_2) defines a unique mesh M such that M_1 and M_2 are its diagonal meshes. We define M to be discrete orthogonal if (M_1, M_2) is rhombic. Consequently, we obtain the following definition:

Table 1. Overview of orthogonal nets studied in this paper.

Additional constraint to an orthogonal mesh	Yields a discrete version of	Features
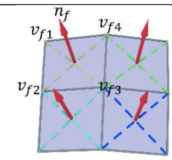 Conjugacy expressed by planar quadrilaterals	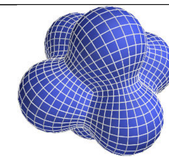 Principal curvature lines	Allows a torsion-free support structure; has nearly rectangular panels; has high visual smoothness (Fig. 8,9,10,11)
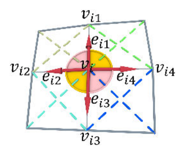 A geodesic net defined by opposite angles being equal	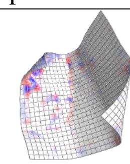 Developable surface	The mesh can be isometrically deformed into the plane and thus be build from planar deformable pieces.
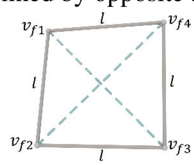 A Chebyshev net defined by constant edge lengths	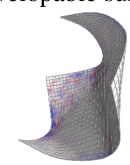 Developable surface	(Fig. 13,14)
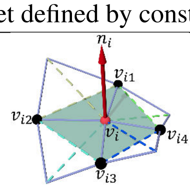 An asymptotic net expressed by planar vertex stars	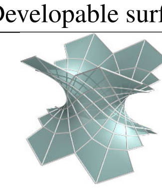 Minimal surfaces	A gridshell with straight lamellas on a minimal surface. (Fig. 15, 16)
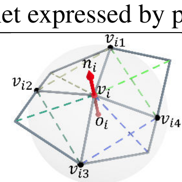 Principal symmetric net expressed by spherical vertex stars	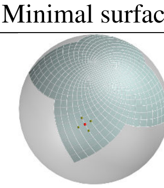 CMC surfaces	A gridshell with circular lamellas on a surface of constant mean curvature. (Fig. 1,17,18)
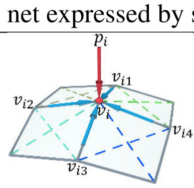 Vertices in equilibrium with vertical loads	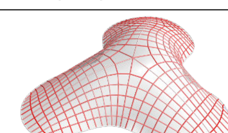 Principal stress net	A gridshell with efficient material usage. (Fig. 19,20)

Definition 3. *The mesh M is orthogonal if and only if the diagonals in every quadrilateral are of equal length.*

Discrete orthogonality manifests itself as well in every quadrilateral through the medial lines, which are the lines connecting midpoints of opposite edges. See Fig. 1 for the relation of an orthogonal mesh, its diagonal meshes and the medial lines.

Lemma 4. *The medial lines of opposite edges in a quadrilateral are orthogonal if and only if the diagonals of the quadrilateral have equal length.*

From a numeric point of view, using medial lines is appealing due to their good approximation properties as the following argument shows. The vertices of a mesh can be seen as the sampling of a smooth surface parametrization $\phi(u, v)$, i.e. $v_{k,l} = \phi(\epsilon k, \epsilon l)$. The edges of the mesh can be seen as discrete tangents. However, they approximate the smooth tangents best at the midpoints $\phi(\epsilon k + \frac{\epsilon}{2}, \epsilon l)$ and $\phi(\epsilon k, \epsilon l + \frac{\epsilon}{2})$ and not at the vertices $v_{k,l} = \phi(\epsilon k, \epsilon l)$. Hence, they are unfavorable for approximating the angle $\measuredangle(\partial_u X(u, v), \partial_v X(u, v))$. In contrast, the two medial lines of the quadrilateral with vertices $v_{k,l}, v_{k+1,l}, v_{k+1,l+1}, v_{k,l+1}$ both approximate the smooth tangents by order $O(\epsilon^2)$ in the same point, namely $\phi(\epsilon k + \frac{\epsilon}{2}, \epsilon l + \frac{\epsilon}{2})$. Therefore, the angle of medial lines approximates the angle of tangents in the smooth parametrization by order $O(\epsilon^2)$ as well. This concept is, of course, not restricted to orthogonal meshes only. Any angle between medial lines could be prescribed, but the concise formulation via diagonal length only works for orthogonality.

One great advantage of this approach is that in contrast to other prominent versions of discrete orthogonal meshes such as circular meshes [2] or conical meshes [3], it works for non-planar quadrilaterals as well. From a Discrete Differential Geometric point of view, meshes with planar quadrilaterals resemble conjugate nets. Hence, the requirement of planarity on top of orthogonality limits the choice of possible nets substantially, as the only curves that are orthogonal and conjugate are the principal curves on a surface (see section 4.1 for more details). Another great advantage is the simplicity of the constraint. As the constraint is only quadratic, standard Gauß-Newton methods for optimization are applicable. Last but not least, this orthogonality constraint still leaves a high degree of freedom for the mesh, which allows the coupling with other constraints as one would expect coming from the smooth theory.

3. Ivory's theorem and orthogonal multi-nets

The famous *Theorem of Ivory* [16] is closely related to our definition of orthogonality.

Theorem 5. *The diagonals in a quadrilateral formed by arcs of confocal conics have equal length (compare Fig. 3).*

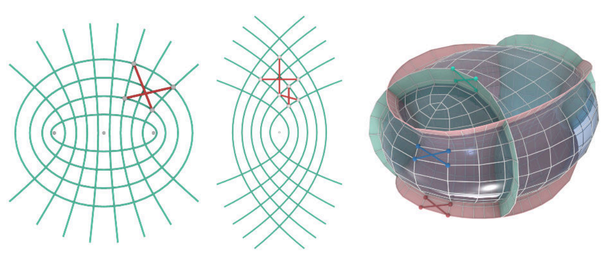

Fig. 3. Ivory's theorem: Diagonals in any quadrilateral formed by confocal conics are of equal length. The same holds true in the system of confocal quadrics.

Ivory's theorem tells us that the intersection points of a family of confocal conics span an orthogonal mesh in the plane. Meshes generated that way exhibit a special kind of orthogonality. Namely, they are discrete orthogonal multi-nets, in the definition of a multi-net according to [17]. This means that the diagonals in any combinatorial rectangle are of equal length:

$$\|v_{k,l} - v_{i,j}\|^2 = \|v_{k,j} - v_{i,l}\|^2 \quad \forall i, j, k, l. \tag{1}$$

One can think of orthogonal multi-nets as being orthogonal independently of the sampling density. If the vertices $\{v_{i,j} : 0 \le i \le m, 0 \le j \le n\}$ form an orthogonal multi-net then any subset of the form $\{v_{i,j} : i \in I, j \in J\}$ for $I \subset \{0, \ldots, m\}$ and $J \subset \{0, \ldots, n\}$ is the vertex-set of an orthogonal mesh as well. This allows for changing the grid-size of the mesh while preserving the orthogonality property.

An orthogonal multi-net is highly over-determined. The existence of such meshes is non-trivial and, in fact, the only orthogonal multi-nets in the plane are the meshes generated by confocal conics. Hence, the parameter lines of any orthogonal multi-net in the plane lie on confocal conics. The situation in three-dimensional space is similar. The only volumetric meshes with the Ivory property in every cell are the ones generated by confocal quadrics [18]. This holds both in the smooth case as well as in the discrete case (see Fig. 3). The only surfaces that allow for a parametrization with the Ivory property are the Liouville surfaces [19]. We can think of an orthogonal multi-net as a discrete version of a Liouville surface with the only difference being that we measure distance in the ambient space and not the geodesic distance inside the surface.

3.1. *Properties of orthogonal multi-nets*

In this section, we give a short analysis of all meshes with the multi-net property that will lead us to an easy construction method. We evaluate Eq. (1) for two rectangles with the same horizontal parameter lines H_j and H_l sharing one vertical edge, i.e. we choose the indices i, j, k_1, l and i, j, k_2, l,

$$\|v_{i,j} - v_{k_1,l}\|^2 = \|v_{i,l} - v_{k_1,j}\|^2,$$
$$\|v_{i,j} - v_{k_2,l}\|^2 = \|v_{i,l} - v_{k_2,j}\|^2.$$

Taking the difference of the two equations yields

$$\begin{aligned} &2v_{i,j} \cdot (v_{k_2,l} - v_{k_1,l}) + \|v_{k_1,l}\|^2 - \|v_{k_2,l}\|^2 \\ =&2v_{i,l} \cdot (v_{k_2,j} - v_{k_1,j}) + \|v_{k_1,j}\|^2 - \|v_{k_2,j}\|^2. \end{aligned}$$

As all quadratic terms of $v_{i,j}$ and $v_{i,l}$ vanish, we can conclude that the same set of affine relations between $v_{i,j}$ and $v_{i,l}$ holds for any value of i. Thus, there is an affine mapping that maps the j-th horizontal parameter line to the l-th horizontal parameter line

$$v_{i,j} = A_{j,l} v_{i,l} + a_{j,l}, \quad A_{j,l} \in \mathbb{R}^{3\times3}, \; a_{j,l} \in \mathbb{R}^3. \tag{2}$$

The same argument can be made for the vertical parameter lines. Expressing $v_{k,l}$ and $v_{i,l}$ by Eq. (2) in Eq. (1), we find that all vertices of the j-th horizontal parameter line meet the same quadratic equation. Hence, the vertices of every horizontal or vertical parameter line lie on a quadric. If we assume one horizontal parameter line not to be planar, we can deduce that $A_{j,l}$ has to be symmetric. Moreover, a coordinate system can always be chosen such that the constant part $a_{j,l}$ in Eq. (2) is zero. Under these assumptions and writing $I \in \mathbb{R}^{3\times3}$ for the identity matrix, we find that

$$v_{i,j}^T (A_{j,l}^2 - I) v_{i,j} = c, \quad \forall i$$
$$v_{i,l}^T (I - A_{j,l}^{-2}) v_{i,l} = c, \quad \forall i.$$

Let x be an eigenvector of $(A_{j,l}^2 - I)$ with corresponding eigenvalue λ, then x is also an eigenvector of $(I - A_{j,l}^{-2})$ with corresponding eigenvalue $\mu = \frac{\lambda}{\lambda+1}$. As the eigenvalues meet $\frac{1}{\mu} - \frac{1}{\lambda} = 1$, the two quadrics defined by the above equations have to be confocal. Therefore, all horizontal parameter lines lie on confocal quadrics. The same holds for all vertical parameter lines. Moreover, if the quadric Q containing a horizontal parameter line H_j is unique, the quadric determines the affine mappings to all other horizontal parameter lines up to the choice of one parameter. Let $Q = \{x \in \mathbb{R}^3 : x^T S x = 1\}$ where S is a symmetric matrix (we will keep this assumption for the rest of the paper). Then, the affine mapping $v_{i,j} \mapsto v_{i,l}$ has to be of the form

$$v_{i,l} = \sqrt{t_l S + I}\, v_{i,j}, \quad t_l \in \mathbb{R}.$$

Note that the square root always exists for t_l sufficiently close to zero. We conclude that an orthogonal multi-net is determined up to sampling size as soon as one polyline on a given quadric is fixed.

3.2. Construction of orthogonal multi-nets

The affine mappings between parameter lines lead to an interactive design of multi-nets. A user can first choose a quadric Q and draw a polyline $\{v_{i0} : 0 \leq i \leq n\}$ on that quadric. If the quadric containing the polyline is unique, the shape of the entire multi-net is already determined by the initial polyline. The multi-net is then given by

$$v_{ij} = \sqrt{t_j S + I}\, v_{i0}$$

for any admissible choice of $t_j \in \mathbb{R}$, compare Fig. 4. One does not have to choose the sampling right away and can instead work with the smooth underlying surface parameterized by

$$\phi(s,t) = \sqrt{tS + I}\, c(s), \;\; s, t \in \mathbb{R},$$

where c is a curve on the quadric Q corresponding to S. Any sampling $v_{ij} = \phi(s_i, t_j)$ of that surface gives an orthogonal multi-net. Hence, the mesh can be made coarser or finer at any time while preserving the (multi) orthogonality property.

Another way to obtain orthogonal multi-nets from a more algebraic input is by using elliptic coordinates. To see that, we observe that the curve $t \mapsto \sqrt{tS + I}\, c(s)$ is the intersection of the two quadrics orthogonal to Q in the system of confocal quadrics of Q that go through $c(s)$. Hence, we can think of orthogonal multi-nets as axis-aligned generalized cylinders in elliptic coordinates. They can be parameterized by e.g.

$$\phi(s,t) = \begin{pmatrix} \pm\sqrt{\frac{(a+\lambda(t))(a+\mu(s))(a+\nu(s))}{(a-b)(a-c)}} \\ \pm\sqrt{\frac{(b+\lambda(t))(b+\mu(s))(b+\nu(s))}{(b-a)(b-c)}} \\ \pm\sqrt{\frac{(c+\lambda(t))(c+\mu(s))(c+\nu(s))}{(c-a)(c-b)}} \end{pmatrix}, \tag{3}$$

where $a > b > c > 0$ and $-a < \nu(s) < -b < \mu(s) < -c < \lambda(t)$. By choosing the functions $\mu(s)$ and $\nu(s)$ one determines a curve on an ellipsoid with axes $\sqrt{a}$, $\sqrt{b}$ and $\sqrt{c}$ for $\lambda = 0$. For different values of λ this curve is transported along the intersection lines of confocal one-sheeted and two-sheeted hyperboloids. One can exchange the role of ellipsoids and hyperboloids by having μ or ν depend on t instead of λ. The different cases are shown in Fig. 4.

Note that for our analysis we assume that at least one parameter line is not planar. Cases where all parameter lines are planar occur in rotational surfaces where the parameter lines follow the meridian curves and the parallel circles [20].

The parametrizations we derive are not principal and in general one cannot expect the quadrilaterals to be close to planar. Multi-nets like the one in Fig. 4 will have highly non-planar faces if λ gets close to μ. Otherwise, faces are sufficiently planar in the sense that they form a good initial guess for optimization towards planarity (see Fig. 10). Thus, in the eyes of the authors, orthogonal multi-nets can be an interesting design tool (see Fig. 5) in e.g. freeform architecture.

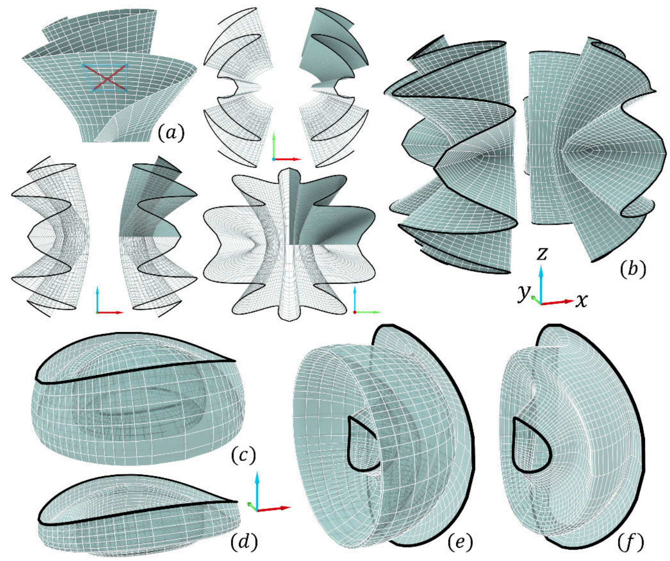

Fig. 4. Orthogonal multi-nets. (a) The mesh is generated by Eq. (3) and extended to (b) by reflection in the coordinate planes. One family of parameter lines lies on confocal ellipsoids. The other family lies on the intersections of confocal one-sheeted and two-sheeted hyperboloids. The meshes (c-f) are different types of orthogonal multi-nets where the role of the confocal quadrics is switched.

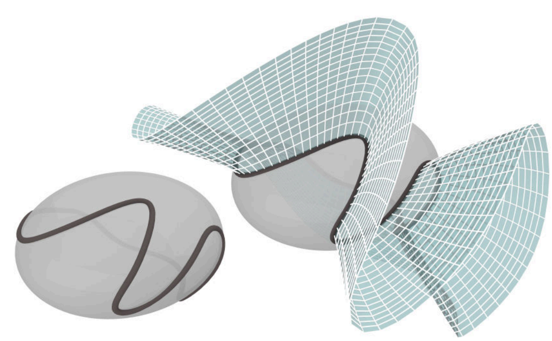

Fig. 5. The multi-net is created interactively. The curve drawn on the ellipsoid determines the entire multi-net up to sampling size.

3.3. Orthogonal multi-nets as regularizers

The relation of orthogonal multi-nets to quadrics suggests using a pseudo multi-net property as regularizer. We propose a regularization method where a mesh is optimized to meet the multi-orthogonality property not globally but locally in every $m \times n$ face patch. While usual regularization constraints force polylines to be straight lines by minimizing the second derivative, we expect this regularization to force polylines towards curves of the form $t \mapsto \sqrt{tS + I}\, v$. We describe the effects of the method in detail in the next section.

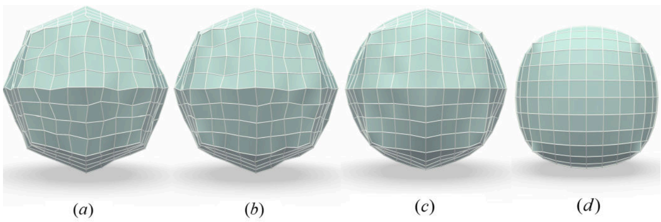

Fig. 6. The effect of multi-net regularization. The mesh (a) is optimized using different energies: E_{ortho} in (b), $E_{ortho} + 0.005E_{multi}$ in (c) and $E_{ortho} + 0.005E_{fair}$ in (d). Optimizing for orthogonality alone is not enough to obtain a smooth net (b). The regularization of E_{multi} helps to obtain smooth polylines while preserving the shape (c). In contrast, including the traditional fairness term E_{fair} leads to a loss of the initial shape (d).

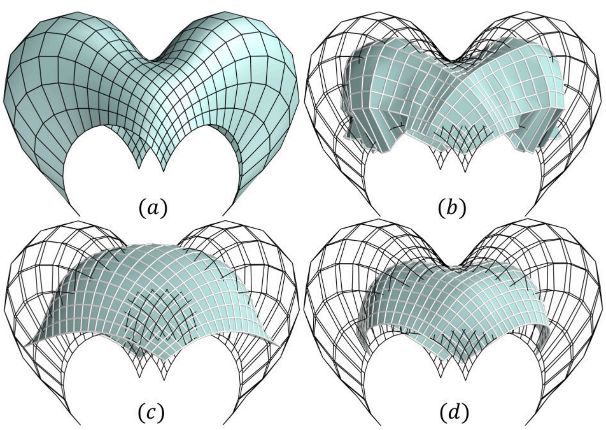

Fig. 7. We optimize mesh (a) using different energies. Using only E_{multi} yields (b). The mesh is still doubly curved but the appearance is not smooth. Using only E_{fair} instead gives a smooth appearance but a loss of features (c). A combination of both Energies gives the mesh (d) with smooth polylines in a doubly curved surface.

4. Applications

In the remainder of this paper we proceed to briefly showcase possible applications of the introduced orthogonality constraint. While we do not go into detail with each method, we hope to convey the versatility of the approach by demonstrating different use-cases. We are not the first to come up with these applications. Principal meshes and discrete principal stress lines were characterized with this orthogonality condition in [15]. Minimal surfaces and constant mean curvature (CMC) surfaces appeared with this orthogonality condition in [14]. The idea to use orthogonal geodesics to characterize developable surfaces is based on [21], but the authors used a different orthogonality constraint.

Computationally, our approach is more or less the same in every use-case. The Discrete Differential Geometric theory defines energy terms which the corresponding structures minimize. The contributions to these energy terms are formed by the local constraints at every vertex star or at every face, compare Tab. 1. Eventually, a weighted sum of energies of the form

$$E = E_{Ortho.} + \lambda E_{\square} + \omega_1 E_{fair} + \omega_2 E_{multi}$$

is minimized. Here, ω_1 and ω_2 are small weights of magnitude approximately 10^{-3}. Different choices for $E_{\square}$ and their geometric meaning are discussed in the following subsections.

The energy term E_{Ortho} is defined as

$$E_{Ortho} = \sum_{f=1}^{|F|} (\|v_{f1} - v_{f3}\|^2 - \|v_{f2} - v_{f4}\|^2)^2.$$

Here $|F|$ is the number of quad faces in the mesh and we index the vertices of a face f by f_i in counter-clockwise order. Minimizing E_{Ortho} leads to equal diagonal length and thus an orthogonal mesh.

Fairness energy terms E_{fair} and E_{multi} are included in every optimization which is essential to keep the interpretation of meshes as discrete versions of smooth nets justified. Both energy terms force lines to be straight. Their weights ω_1 and ω_2 are set to zero in the final iterations of optimization as the respective energies do not converge to zero in general.

The term E_{fair} is a classical fairness term defined as

$$E_{fair} = \sum_{i \in polyline} (2v_i - v_{il} - v_{ir})^2.$$

Here v_{il}, v_i, v_{ir} are three consecutive vertices on a parameter line. Minimizing E_{fair} can be seen as minimizing the second derivative of the parameter lines.

The term E_{multi} expresses the pseudo multi-net property. It expands E_{Ortho} to every one-by-two face patch and rewards straight lines and orthogonality at the same time. As the pseudo multi-net property implies local orthogonality, this fairness term is only applicable for orthogonal meshes. However, it should be mentioned that E_{multi} alone would be too weak to guarantee useful outcomes of the optimization which is why E_{fair} is always needed. In contrast, using E_{fair} without E_{multi} still gives reasonable results. The advantage of E_{multi} is that it has less influence on the entire shape of the mesh than E_{fair}. Certain features like doubly curved areas or crisp creases in a mesh get easily lost if E_{fair} is minimized. Giving less weight to E_{fair} and adding E_{multi} instead can help in such situations as we show in Fig. 6 and Fig. 7.

To solve the optimization problem we use the regularized Gauß-Newton algorithm as described in [22, 23]. Approximately ten to fifty iterations are done in our optimizations. It is important that an initial guess is guided by some geometric intuition; otherwise, one cannot hope to receive a useful outcome.

4.1. *Principal meshes*

The so called *principal curvature lines* are a special family of curves on a surface. They follow the directions in which a surface is maximally or minimally bent. These directions are always orthogonal and conjugate regardless of the surface. The reverse is also true: Any net that is conjugate and orthogonal is a net of principal curvature lines.

While the concept of orthogonality is clear, the concept of conjugacy can be a bit harder to grasp geometrically. It means that the tangents of curves of the first parameter family where the curves intersect a given curve of the second parameter family, form a developable surface. On an infinitesimal scale we can think of this as neighbouring tangents being coplanar. Hence, on an infinitesimal scale conjugate curves form planar quadrilaterals. This infinitesimal planarity carries over to the discrete case where we call a quad mesh conjugate if all its faces are planar. In our approach a principal mesh is thus an *orthogonal quad mesh with planar faces*, compare Tab. 1.

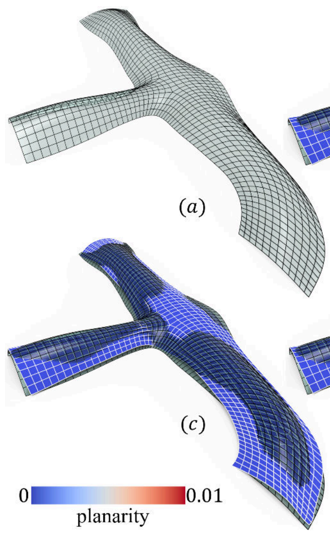

Fig. 8. Different discrete principal curvature lines. The mesh (a) is optimized to be a circular mesh (b), conical mesh (c) and a principal mesh in our sense (d). All optimizations were performed with equal weights and exhibit almost perfectly planar faces. The face colors range from blue to red according to the evaluated planarity, which is the relative spacial distance between two diagonal lines.

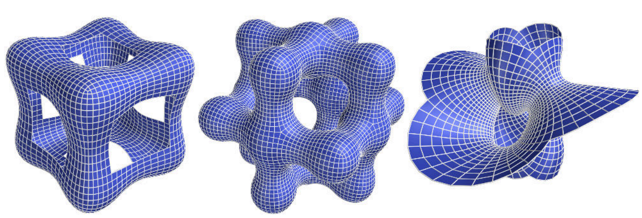

Fig. 9. Principal curvature line meshes. The meshes are optimized to have planar and orthogonal faces.

Quad meshes aligned with principal curvature lines have good visual properties. In [24], the authors concluded that these meshes are best suited to optimize visual fairness defined via a small variation of the normal vector, compare Fig. 10. Principal curvature meshes are particularly relevant in freeform architecture (see [1] for a detailed discussion). On the one hand, they provide a reliable way to approximate a smooth surface with planar quadrilaterals that are close to rectangles which is preferable from a visual perspective as well as from the view point of cost effective realization. On the other hand, they allow a torsion-free support structure as the normals along principal curvature lines form developable surfaces, compare Fig. 11. This property is best captured through circular meshes [2] or conical meshes [3], which allow an offset-mesh with parallel

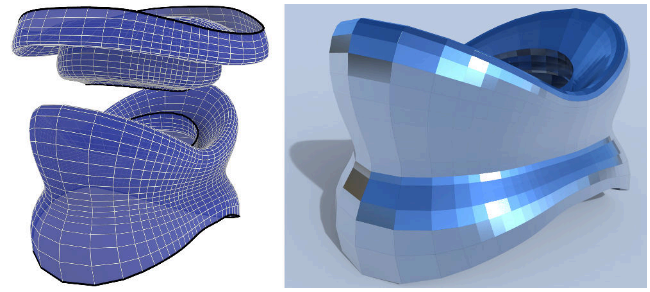

Fig. 10. We use the multi-nets as inspiration for new designs of principal meshes. The mesh from Fig. 4-(f) is optimized to be principal giving the mesh at the top left. A Möbius transformation gives the mesh on the bottom left and maintains the principal mesh properties with high accuracy. The mesh on the right is a rendering of the same mesh as a reflective surface with high visual smoothness [24].

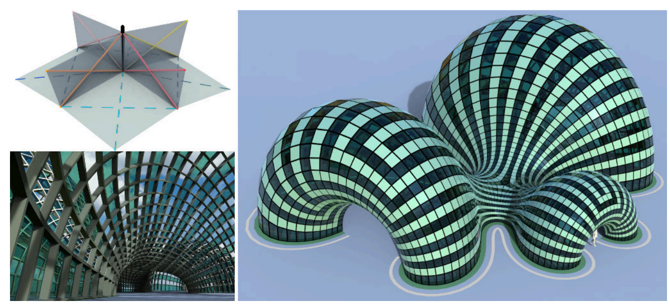

Fig. 11. Principal curvature lines give rise to torsion-free support structures. The top-left picture shows a torsion-free node where orthogonal and close to planar quadrilaterals meet in a common line. The right picture shows an architectural roof which allows a construction from torsion-free beams of constant height (bottom left).

edges and constant face or vertex distance, respectively. We obtain principal meshes that behave similar to circular or conical meshes (Fig. 8).

Computationally, planarity of faces can be expressed by the energy term

$$E_{PQ} = \sum_{f=1}^{|F|} \sum_{j=1}^{4} (n_f \cdot (v_{fj} - v_{fk}))^2 + \sum_{f=1}^{|F|} (n_f \cdot n_f - 1)^2,$$

where the index $k = j \mod 4 + 1$. The face normals n_f are introduced as auxiliary variables, compare [22]. In Fig. 9, we demonstrate principal meshes obtained by our method. The faces are planar and orthogonal with high accuracy at the same time.

4.2. *Developable surfaces via orthogonal geodesic nets*

Developable surfaces are surfaces with zero Gaußian curvature. They can, at least locally, be isometrically deformed into the plane. Thus, they are particularly interesting for manufacturing as developable shapes can be produced by bending flat pieces. Certain families of curves like orthogonal geodesic nets or isogonal Chebyshev nets only exist in developable surfaces. This can be used to model developable surfaces as it was done in [21, 25] using orthogonal geodesics. We present two similar approaches, one using orthogonal geodesic nets and one using orthogonal Chebyshev nets. In the smooth setting these nets would be equivalent but their discretizations yield slightly different structures.

Geodesics are locally the shortest path between two points in a surface. They do not bend from the point of view of the surface. This means that the orthogonal projection of a geodesic $c : \mathbb{R} \to \mathbb{R}^3$ around a point $P = c(t_0)$ to the tangent plane in P has zero curvature in P. This is equivalent to the geodesic curvature of c being zero. Geodesics can be thought of as the straight lines on a surface. A particle that moves freely along a surface with no forces acting on the particle except for the ones that keep it on the surface, moves along a geodesic with constant speed. Thus, geodesics are of special interest in physics.

A discrete counterpart of geodesics was introduced in [26] in order to discretize surfaces of constant negative Gaußian curvature. There, a discrete geodesics net is defined as a quad mesh where opposite angles at every vertex star are equal. In [21, 25], the concept of discrete geodesics was expanded to orthogonal geodesics by requiring that all four angles at every vertex star are equal. Alternatively, one can use the orthogonality constraint presented in this paper obtaining the following definition.

Definition 6. *An orthogonal geodesic mesh is a quadrilateral mesh where diagonals in every face have equal length and opposite angles at every vertex star of valence four are equal (see Tab. 1).*

The energy term we use to create geodesic meshes is

$$E_{Gnet} = \sum_{i=1}^{|V|} \left((e_{i1} \cdot e_{i2} - e_{i3} \cdot e_{i4})^2 + (e_{i2} \cdot e_{i3} - e_{i4} \cdot e_{i1})^2\right) + \sum_{i=1}^{|V|} \sum_{j=1}^{4} \left(e_{ij} - \frac{v_{ij} - v_i}{||v_{ij} - v_i||} \right)^2,$$

where e_{ij} are the unit edge vectors emanating from a vertex v_i. They are introduced as auxiliary variables in the optimization. We index the neighbours of vertex v_i by v_{ij}. The value $||v_{ij} - v_i||$ is assumed constant when the gradient is computed and updated after every iteration.

Another way to obtain developable surfaces is to discretize orthogonal Chebyshev nets. A smooth Chebyshev net ϕ satisfies $\partial_u ||\partial_v \phi||^2 = \partial_v ||\partial_u \phi||^2 = 0$. This can be seen as the infinitesimal quads formed by the net having constant v-length along every u-parameter line and vice versa. The discrete version of Chebyshev nets are quad meshes where opposite edges in every quadrilateral have equal length [2]. It is always possible to reparameterize a smooth Chebyshev net such that $||\partial_u \phi|| = ||\partial_v \phi|| = 1$. The Gaußian curvature of the parameterized surface can then be computed from the angle $\alpha = \measuredangle(\partial_u \phi, \partial_v \phi)$ by $K = -\frac{\alpha_{uv}}{\sin \alpha}$ ([27]). Consequently, a Chebyshev net where α is constant has to lie on a developable surface. We can discretize the special case of an orthogonal Chebyshev net with $||\partial_u \phi|| = ||\partial_v \phi|| = 1$ in the following way.

Definition 7. *A quadrilateral mesh is a Chebyshev net if all edges are of equal length. If the Chebyshev net is orthogonal, it constitutes a discrete developable surface.*

A single quadrilateral in a Chebyshev net has many interesting properties. The four triangles formed by any three of its vertices are all congruent. Consequently, every quadrilateral is symmetric with respect to reflection in its medial lines. Hence, the medial line connecting m_1 in Fig. 12 lies in the symmetry plane of v_1 and v_2 and also in the symmetry plane of v_3 and v_4. Therefore, the medial lines meet the edges of the quadrilateral at right angles. Two consecutive medial lines lie in the symmetry plane of the edge that both medial lines intersect, see Fig. 12. This allows us to view the polylines formed by midpoint connectors as discrete geodesics. Consider the situation in Fig. 12 right. A reasonable discrete tangent plane in p_2 contains the edge e_{34}. It is orthogonal to the osculating plane of the polyline through p_1, p_2 and p_3. Like in the smooth case, the orthogonal projection of the polyline to the tangent plane is straight. In smooth differential geometry any Chebyshev net is also an orthogonal geodesic net and vice versa. We have found a discrete version of this fact.

Lemma 8. *The polylines formed by the midpoint connectors of an orthogonal Chebyshev net constitute an orthogonal geodesic net.*

These geodesics also have the property of being locally the shortest paths. Consider again the situation of Fig. 12: The shortest path from p_1 to p_3 that crosses e_{43} is indeed the path through p_2.

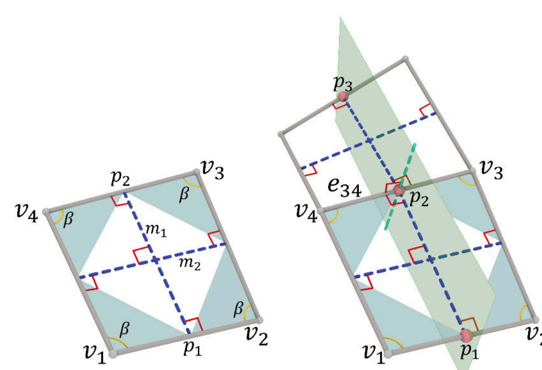

Fig. 12. ***Left:*** **An orthogonal Chebyshev quadrilateral. All edges have equal length. So do the midpoint connectors and the diagonals. The medial lines meet the edges of the quadrilateral in right angles.** ***Right:*** **The plane spanned by the vertices p_1, p_2 and p_3 is orthogonal to e_{34}. Thus, the polylines formed by midpoint connectors can be seen as discrete geodesics.**

The energy term characterizing Chebyshev nets in our optimization is

$$E_{Cheby} = \sum_{e_{ij}}^{|E|} ((v_i - v_j)^2 - l^2)^2,$$

where v_i, v_j are endpoints of an edge e_{ij} from $|E|$ edges and l is a variable or an assigned value. Optimizing a mesh to minimize $E_{Gnet} + E_{Ortho}$ or $E_{Cheby} + E_{ortho}$ gives the result seen in Fig. 13 and Fig. 14. We find that the Gaußian curvature is close to zero and the normal image is close to being one-dimensional.

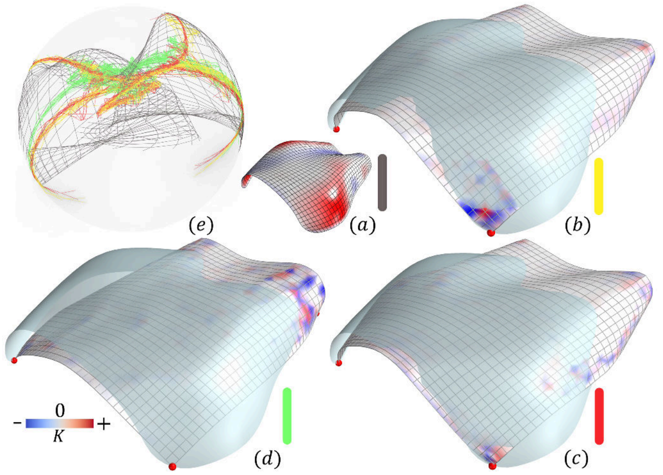

Fig. 13. We optimize an initial mesh (a) to be developable using the method of [21] in (b), using orthogonal G-nets in our sense in (c) and using orthogonal Chebyshev nets in (d). The four corner vertices are fixed for each mesh. All meshes are close to developable surface whose Gaußian image has nearly vanishing area as shown in (e).

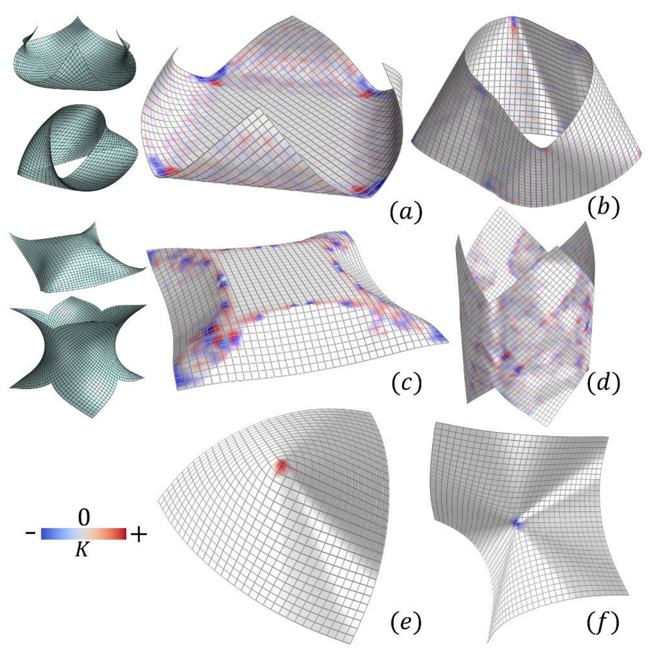

Fig. 14. Different developable meshes colored by Gaußian curvature K. The initial meshes for the optimization are depicted in green next to the developable meshes. For (a) and (b) orthogonal geodesics were used and for (c) and (d) orthogonal Chebyshev nets. The meshes (e) and (f) are orthogonal geodesic nets and Chebyshev nets at the same time.

4.3. Minimal surfaces via orthogonal asymptotic nets

After conjugate curves and geodesics, we focus on *asymptotic curves* as the next classical example of families of curves. These are the curves of zero torsion, i.e. the derivative of the normal vector along an asymptotic curve is always orthogonal to the tangent vector of the curve. Another definition that is more prone to discretization is that the osculating plane of an asymptotic curve in a point P is the tangent plane of the surface at that point. Consequently, two intersecting asymptotic curves have to have identical osculating planes in the point of intersection. The discrete osculating plane of a polyline in a point P is just the plane spanned by P and its two neighbours in the polyline. Thus, asymptotic meshes can be defined as those quadrilateral meshes where every vertex star is planar. This definition has first been introduced in [28, 29] and is predominant in the field of Discrete Differential Geometry [2].

The angle 2α of two asymptotic curves is connected to the principal curvatures κ_1 and κ_2 by $\tan^2(\alpha) = -\kappa_1/\kappa_2$. Thus, an asymptotic net that is orthogonal as well implies $\kappa_1 + \kappa_2 = 0$, so it has to be the parametrization of a *minimal surface*. Minimal surfaces have been studied extensively in the smooth setting as well as in the discrete setting and are still a vivid field of research. By combining our orthogonality condition with the classic asymptotic condition of planar vertex-stars, we obtain a new model of discrete minimal surfaces (see Fig. 15 and Fig. 16). To be more precise, we obtain an asymptotic parametrization of a minimal surface.

The planes along any curve on a surface defined by the surface normal and the tangent of the curve envelop a developable surface. The normal curvature of the curve in the initial surface corresponds to the geodesic curvature in the developable surface. Thus, an asymptotic parametrization of a surface can be used for a physical gridshell model of a minimal surface with planar developable strips (see Fig. 16).

The energy term we need to minimize to obtain planar vertex stars is

$$E_{Anet} = \sum_{i=1}^{|V|} \sum_{j=1}^{4} (n_i \cdot (v_{ij} - v_i))^2 + \sum_{i=1}^{|V|} (n_i \cdot n_i - 1)^2,$$

where the auxiliary variable n_i stands for the normal at vertex v_i. Minimizing $E_{Ortho} + E_{Anet}$ yields the results seen in Fig. 15 and Fig. 16.

4.4. Constant mean curvature (CMC) surfaces via orthogonal S-nets.

The so-called *principal symmetric meshes (S-nets)* are generalizations of asymptotic curves introduced in [31, 32] and studied in great detail in [33]. They can be characterized by the fact that the principal curvature lines bisect the principal symmetric curves in every point. The normal curvature of a line is determined by the angle α which the curve forms with the first principal direction by the *Euler formula* $\kappa_n = \cos(\alpha)^2\kappa_1 + \sin(\alpha)^2\kappa_2$. Hence, two principal symmetric curves have equal normal curvature in their point of intersection. The normal curvature of a curve c at a point p determines the so-called *Meusnier sphere* (see e.g. [34]), a sphere with tangential contact to the surface in p and radius $1/\kappa_n$. The osculating circle of every curve through p with the same tangent as c lies on the *Meusnier sphere*. Consequently, the osculating circles of two principal symmetric curves in their point of intersection lie on the same sphere since their *Meusnier spheres* coincide. This suggests the discretization of principal symmetric meshes developed in [31, 33]:

Definition 9. *A quadrilateral mesh is called principal symmetric if the five points of every vertex star lie on a common sphere.*

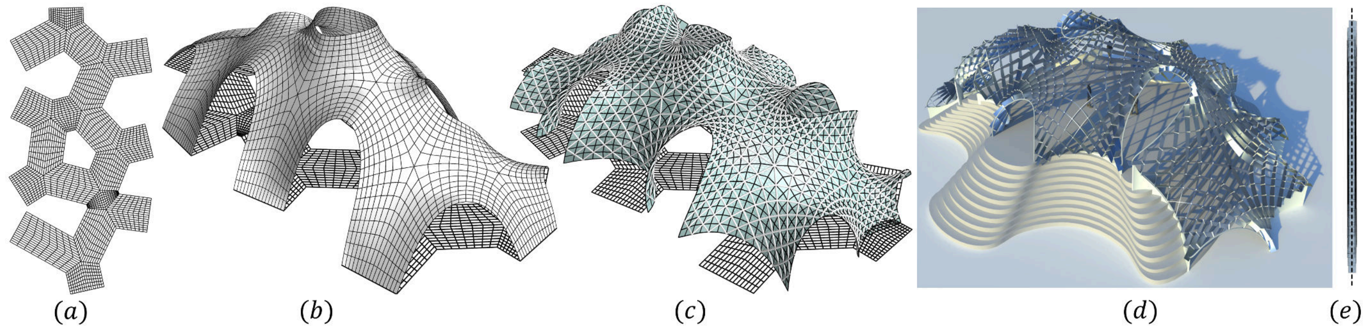

Fig. 15. Modeling a minimal gridshell. We start with a flat mesh (a). By using the form-finding software [30] we obtain a membrane mesh (b) that is floated up from (a). The corresponding diagonal mesh is optimized to be an orthogonal asymptotic net (c). In (d) we see the final rendering of the mesh as a minimal gridshell. The unrollments of the individual developable strips are straight (e).

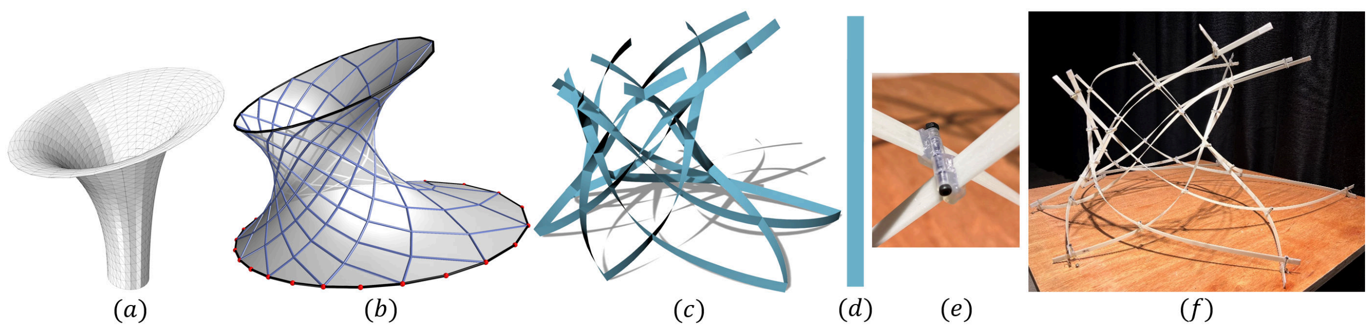

Fig. 16. Computational design and construction pipeline of a minimal gridshell. In (a) we extract a quad mesh from a given triangular mesh as an initial mesh. In (b) we optimize it to be an orthogonal asymptotic net with bottom points gliding on the xy−plane. (c) is the asymptotic gridshell formed by the developable strips along the asymptotic lines. The individual strips enroll as straight lines in the plane (d). (f) is a physical realization of the model with repetitive 3D printed joints (e).

If principal symmetric curves are orthogonal, they form an angle of 45° with the principal curvature lines and the normal curvature equals the mean curvature of the surface. As the mean curvature is the same as the radius of the *Meusnier sphere* in this case, we obtain a discrete model for CMC surfaces by requiring constant radius of the spheres at the vertex stars.

Definition 10. *A quadrilateral mesh is a discrete CMC surface, if it is orthogonal and spheres at the vertex stars have constant radius.*

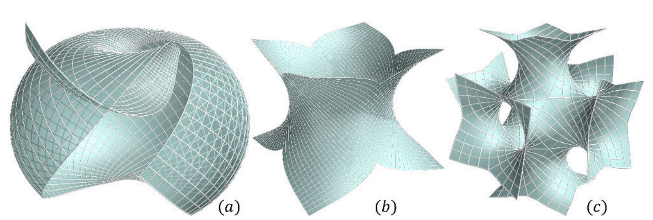

Fig. 17. Discrete CMC surfaces. Each mesh is optimized to be a discrete orthogonal S-net with constant radius of the Meusnier spheres.

The developable strips along orthogonal S-nets exhibit useful features similar to the asymptotic case. If the normal curvature along a line is constant, the geodesic curvature of the line in the corresponding developable strip is also constant. Therefore, the

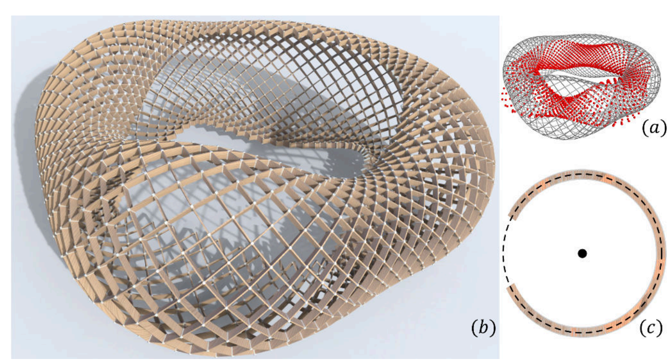

Fig. 18. (a) Orthogonal S-net with constant radius 3.5 of the Meusnier spheres at all vertices. The sphere centers are drawn as red dots. (b) An orthogonal gridshell based on the S-net. (c) The unrollments of all circular strips in the plane nearly align along a circle of radius 3.5.

developable strips along an orthogonal S-nets on cmc surfaces are all isometric to sections of the same ring.

Computationally, we enforce the S-net property via the energy term

$$E_{S\,net} = \sum_{i=1}^{|V|} \sum_{j=1}^{4} ((v_{ij} - o_i)^2 - R^2)^2 + \sum_{i=1}^{|V|} ((v_i - o_i)^2 - R^2)^2,$$

where the sphere centers o_i and the radius R are introduced as auxiliary variables. The radius R can be prescribed with a given number to determine the mean curvature of the mesh. The results of minimizing $E_{Snet}+E_{Ortho}$ are seen in Fig. 17 and Fig. 18.

4.5. Principal stress nets

Orthogonality does not only appear in geometric shapes but also in physical structures. If the quadrilateral mesh describes a load bearing structure, forces act along the edges of the mesh. The mesh is in equilibrium if the sum of the forces at each vertex is zero. This means that in a physical realization of the mesh no bending forces appear. As described in [35], a quadrilateral mesh in equilibrium that additionally is orthogonal, is a discrete version of the *net of principal stress lines* in the surface. Under certain assumptions, [36] showed that the optimal orientation of fibres in a filamentary composite is along the lines of principal stress. Architectural self supporting structures where beams follow principal stress lines are regarded as using material very efficient [37]. Alas, a precise statement about optimality is hard to make. We do not go into detail here.

If a vertical load p_i is applied in an unsupported vertex v_i, the equilibrium condition in v_i reads

$$c_{load,i} := \sum_{j=1}^{4} w_{ij}(v_i - v_{ij}) - \begin{bmatrix} 0 \\ 0 \\ p_i \end{bmatrix} = \begin{bmatrix} 0 \\ 0 \\ 0 \end{bmatrix}.$$

Here the sum is over neighbouring vertices of v_i and w_{ij} denotes the force density in the edge from v_i to v_j. The force densities are introduced as auxiliary variables and meet $w_{ij} = -w_{ji}$. The vertical load p_i can depend on the mesh in which case we update it after every iteration. We obtain equilibrium by minimizing the energy term

$$E_{Equi} := \sum_{i=1}^{|V|} c_{load,i}^2, \tag{4}$$

where the sum is only taken over unsupported vertices. The results of our optimization are presented in Fig. 19 and Fig. 20.

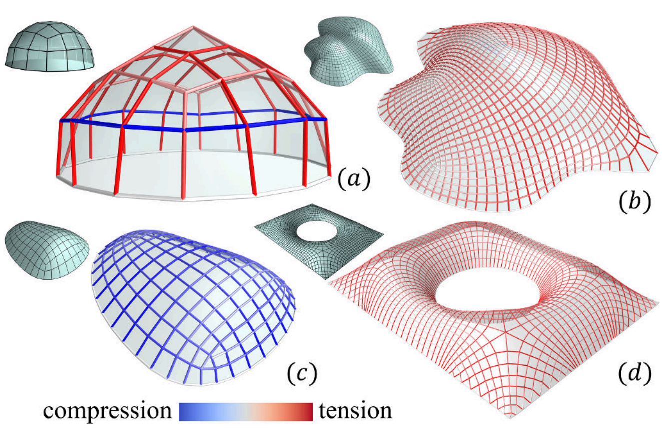

Fig. 19. Orthogonal meshes in static equilibrium under vertical loads with supported boundaries. Inner vertices are unsupported and each of them satisfies the equilibrium Eq. (4). The light green meshes are the initial ones.

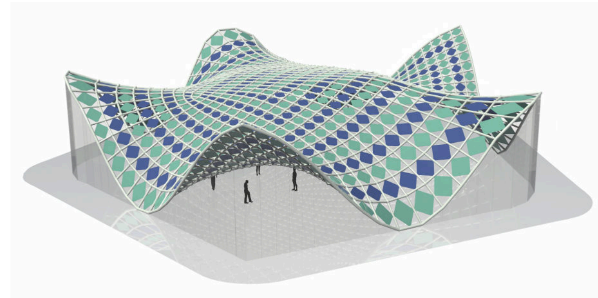

Fig. 20. An architectural rendering of a self supported structure following principal stress lines. The individual faces are decorated with parallelograms of light-weight lamella.

Interactive Design. All presented models allow an interactive design. A user can influence the meshes by manually moving specified handles of the mesh. A dragging energy is then introduced that punishes the distance of the handle to the corresponding vertex of the mesh. One can introduce an additional energy term E_{iso} which guarantees only isometric deformations of the mesh, see [38]. This is particularly useful when working with developable surfaces. The results are seen in Fig. 21.

The computational statistics depend on the quality of the initializations and the complexity of the meshes. In Tab. 2, we list the number of vertices $|V|$, quad faces $|F|$, variables $\#var$ and constraints $\#cons$, and running time per iteration of the interactive design results in Fig. 21. The value ω_{iso} is the weight of the isometric deformation energy E_{iso} in the optimization.

Table 2. Optimization statistics of the interactive design results in Fig. 21 tested on an Intel Xeon E5-2687W 3.0 GHz processor.

Fig. 21	$\lvert V\rvert$	$\lvert F\rvert$	$\#var$	$\#cons$	ω_{iso}	time[s]/it
(a)	1792	1856	11328	18176	0	0.29
(b)	720	768	20115	24960	1	0.34
(c)	2079	2304	82126	96049	0.01	1.26
(d)	2301	2400	42019	50525	0	1.74
(e)	1029	1076	9951	23875	0	0.36

5. Conclusion

In this paper we discuss a discrete version of orthogonality first introduced by [14]. It is expressed by the two diagonals in every quadrilateral being of equal length. We motivate this approach through the theory of mesh pairings. Like in the smooth theory a mesh is called orthogonal if and only if the diagonal meshes are rhombic in the sense of a mesh pairing.

We find that orthogonal multi-nets exist based on *Ivory's Theorem*. These are meshes where every parameter rectangle is orthogonal. We extend *Ivory's Theorem* to three-dimensional space to describe the shape of orthogonal multi-nets and present ways to construct them interactively and analytically.

The orthogonality condition described in this paper is particularly well suited for optimization. Moreover, it is applicable in

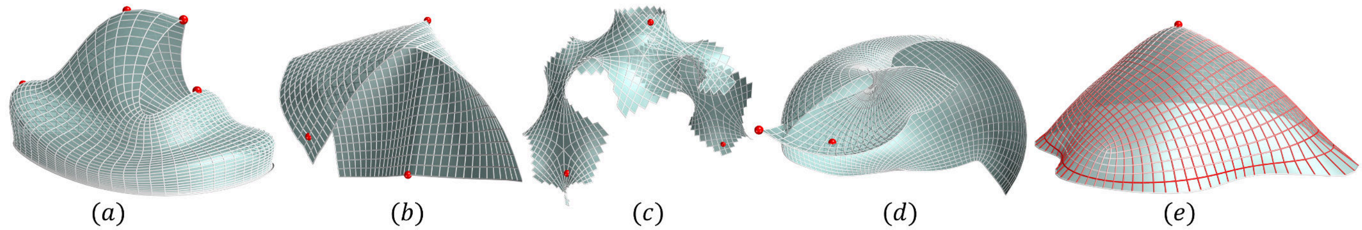

Fig. 21. The different meshes described in this paper can be incorporated in an interactive design process, where a user may change the appearance by dragging the red vertices. The figures show from left to right a principal mesh, developable surface, minimal surface, CMC surface, and a mesh of principal stress lines. The corresponding initial meshes are Fig. 4-(d),14-(e), 15-(c), 17-(a), and 19-(b). In (b) we use the isometric deformation described in [38].

a wide range of applications as it is not limited to planar quadrilaterals. We showcase the versatility of the approach by collecting different ideas where this orthogonality has been used and add the case of orthogonal geodesics and orthogonal Chebyshev nets. Different design pipelines and an interactive design based on the orthogonality constraint are illustrated.

References

[1] Pottmann, H, Eigensatz, M, Vaxman, A, Wallner, J. Architectural geometry. Computers and Graphics 2015;47:145–164.

[2] Bobenko, AI, Suris, YB. Discrete differential geometry. Integrable structure; vol. 98 of *Graduate Studies in Mathematics*. American Mathematical Society, Providence, RI; 2008.

[3] Liu, Y, Pottmann, H, Wallner, J, Yang, YL, Wang, W. Geometric modeling with conical meshes and developable surfaces. ACM Trans Graphics 2006;25(3):681–689.

[4] Bobenko, AI, Schief, WK, Suris, YB, Techter, J. On a discretization of confocal quadrics. i. an integrable systems approach. Journal of Integrable Systems 2016;1(1).

[5] Bobenko, AI, Schief, WK, Suris, YB, Techter, J. On a discretization of confocal quadrics. a geometric approach to general parametrizations. International Mathematics Research Notices 2018;2020(24):10180–10230.

[6] Jiang, C, Peng, CH, Wonka, P, Pottmann, H. Checkerboard patterns with black rectangles. ACM Trans Graphics 2019;38(6):171:1–171:13.

[7] Jiang, C, Wang, C, Schling, E, Pottmann, H. Computational design and optimization of quad meshes based on diagonal meshes. In: Advances in Architectural Geometry 2020. Presses des Ponts; 2021, p. 38–60.

[8] Kenyon, R. The Laplacian and Dirac operators on critical planar graphs. Inventiones mathematicae 2002;150(2):409–439.

[9] Dellinger, F. Discrete isothermic nets based on checkerboard patterns. Discrete and Computational Geometry 2023;forthcoming.

[10] Techter, J. Discrete confocal quadrics and checkerboard incircular nets. Ph.D. thesis; TU Berlin; 2020.

[11] Koenigs, G. Sur les réseaux plans à invariants égaux et les lignes asymptotiques. Comptes Rendus de l´Academie des Sciences, Série 1: Mathématique 1892;114:55–57.

[12] Bobenko, AI, Suris, YB. Discrete koenigs nets and discrete isothermic surfaces. International Mathematics Research Notices 2009;2009(11):1976–2012.

[13] Doliwa, A. Geometric discretization of the Koenigs nets. Journal of Mathematical Physics 2003;44:2234–2249.

[14] Wang, H, Pottmann, H. Characteristic parameterizations of surfaces with a constant ratio of principal curvatures. Comp-Aided Geometric Design 2022;93.

[15] Wang, C, Jiang, C, Wang, H, Tellier, X, Pottmann, H. Architectural structures from quad meshes with planar parameter lines. Computer Aided Design 2023;156.

[16] Ivory, J. On the attractions of homogeneous ellipsoids. Philosophical Transactions of the Royal Society of London 1809;(99):345–372.

[17] Bobenko, A, Pottmann, H, Rörig, T. Multi-nets: Classification of discrete and smooth surfaces with characteristic properties on arbitrary parameter rectangles. Discrete and Computational Geometry 2020;63:624–655.

[18] Blaschke, W. Eine verallgemeinerung der theorie der konfokalen F2. Mathematische Zeitschrift 1928;27:653–668.

[19] Zwirner, K. Orthogonalsysteme, in denen Ivorys Theorem gilt; vol. 5. 1927.

[20] Wang, H, Pellis, D, Rist, F, Pottmann, H, Müller, C. Discrete geodesic parallel coordinates. ACM Transactions on Graphics (TOG) 2019;38(6):1–13.

[21] Rabinovich, M, Hoffmann, T, Sorkine-Hornung, O. Discrete geodesic nets for modeling developable surfaces. ACM Trans Graph 2018;37(2):16:1–16:17.

[22] Tang, C, Sun, X, Gomes, A, Wallner, J, Pottmann, H. Form-finding with polyhedral meshes made simple. ACM Trans Graph 2014;33(4):70:1–70:9.

[23] Jiang, C, Pottmann, H. Optimizing shapes and structures for freeform architecture. In: Baustatik-Baupraxis 14. Universität Stuttgart; 2020, p. 747–754.

[24] Pellis, D, Kilian, M, Dellinger, F, Wallner, J, Pottmann, H. Visual smoothness of polyhedral surfaces. ACM Trans Graphics 2019;38(4):260:1–260:11.

[25] Rabinovich, M, Hoffmann, T, Sorkine-Hornung, O. The shape space of discrete orthogonal geodesic nets. ACM Trans Graph 2018;37(6):228:1–228:17.

[26] Wunderlich, W. Zur Differenzengeometrie der Flächen konstanter negativer Krümmung. Österreich Akad Wiss Math-Nat Kl S-B IIa 1951;160:39–77.

[27] do Carmo, M. Differential Geometry of Curves and Surfaces. Prentice-Hall; 1976.

[28] Sauer, R. Projektive Liniengeometrie. Walter de Gruyter & Co.; 1937.

[29] Sauer, R. Differenzengeometrie. Springer; 1970.

[30] Piker, D. Kangaroo: form finding with computational physics. Architectural Design 2013;83(2):136–137.

[31] Schling, E, Kilian, M, Wang, H, Schikore, D, Pottmann, H. Design and construction of curved support structures with repetitive parameters. In: et al., LH, editor. Adv. in Architectural Geometry. Klein Publ. Ltd; 2018, p. 140–165.

[32] Kilian, M, Wang, H, Schling, E, Schikore, J, Pottmann, H. Curved support structures and meshes with spherical vertex stars. In: ACM SIGGRAPH 2018 Posters. SIGGRAPH '18; New York, NY, USA: Association for Computing Machinery; 2018,.

[33] Pellis, D, Wang, H, Rist, F, Kilian, M, Pottmann, H, Müller, C. Principal symmetric meshes. ACM Trans Graphics 2020;39(4). Proc. SIGGRAPH.

[34] Blaschke, W, Leichtweiß, K. Elementare Differentialgeometrie. Die Grundlehren der mathematischen Wissenschaften; Springer-Verlag; 1973. ISBN 9780387058894.

[35] Kilian, M, Pellis, D, Wallner, J, Pottmann, H. Material-minimizing forms and structures. ACM Trans Graphics 2017;36(6). Proc. SIGGRAPH Asia.

[36] Brandmaier, HE. Optimum filament orientation criteria. Journal of Composite Materials 1970;4:422–425.

[37] Mitchell, T. A limit of economy of material in shell structures. Ph.D. thesis; UC Berkeley; 2013.

[38] Jiang, C, Wang, H, Ceballos Inza, V, Dellinger, F, Rist, F, Wallner, J, et al. Using isometries for computational design and fabrication. ACM Trans Graph 2021;40(4):42:1–12.